# scientific reports



# **OPEN**

# Downregulation of UDP-glucose 6-dehydrogenase predicts adverse outcomes in patients with colorectal cancer and promotes tumorigenesis

Mengyuan Wang<sup>1,6</sup>, Zhiming Ge<sup>1,6</sup>, Xianxian Fan<sup>1</sup>, Hongbo Zhao<sup>1</sup>, Zhenfu Shi<sup>1</sup>, Jiucun Zhang<sup>2</sup>, Li Jin<sup>1</sup>, Yan Li<sup>3</sup>, Jie Wang<sup>1</sup>, Xiaobin Zao<sup>4,5 $\boxtimes$ </sup> & Yun Yang<sup>1 $\boxtimes$ </sup>

UDP-glucose 6-dehydrogenase (UGDH) is the key enzyme of glucuronic acid metabolism and a key mediator in several cancer developmental signaling pathways. However, the expression and function of UGDH in colorectal cancer (CRC) are unclear. Bioinformatics analysis was conducted to research the expression, diagnosis, prognosis, functional enrichment, genetic alterations, and immune characteristics of UGDH in CRC. Hematoxylin-Eosin staining, KI67 immunohistochemistry staining, and UGDH immunohistochemistry staining of clinical colon tissues were performed. The UGDH gene was knocked down in HCT-8 cells. CCK8 and cell wound scratch assays were further performed in UGDH wild-type and UGDH-knockdown HCT-8 cells. UGDH is markedly downregulated in CRC tissues compared to normal tissues, which predicts a poor prognosis. The lower expression of UGDH is associated with a high gene promoter methylation level and genome deletion. UGDH expression is proportional to immune cell infiltration and immune-related genes. UGDH expression is correlated with the p53 signaling pathway. Knockdown of UGDH in HCT-8 cells promoted their proliferation and migration ability. UGDH could be useful as a valuable prognostic biomarker and potential therapeutic target in CRC. UGDH could inhibit the proliferation and migration of CRC cells.

**Keywords** UDP-glucose 6-dehydrogenase, Colorectal cancer, Prognostic marker, Bioinformatics, p53 signaling pathway

Nowadays, cancer has been acknowledged as one of the most prevalent causes of mortality on a global scale<sup>1</sup>, and the issue of tumor drug resistance has become more prevalent<sup>2</sup>. The latest understanding demonstrates that cancer is characterized by metabolic reprogramming, which means cancer cells will alter their metabolic state in response to proliferative signals transmitted by oncogene signaling pathways<sup>3</sup>. The specific microenvironment and metabolites further influence the metabolic phenotype of tumor cells, affecting the immune microenvironment, tumor progression, treatment, and prognosis<sup>4</sup>. According to recent research, uridine diphosphate glucuronic (UDP) acid metabolism is vital during cancer development, which has been identified as a therapeutic vulnerability in a sugar nucleotide biosynthetic pathway that can be exploited in cancer cells with only a limited impact on normal cells<sup>5</sup>.

UDP-glucose 6-dehydrogenase (UGDH) is an oxidoreductase that catalyzes the NAD<sup>+</sup>-dependent four-electron oxidation of UDP-glucose to UDP-glucuronic acid<sup>6</sup>. The active site of UGDH contains a highly conserved cysteine residue, which plays a key role in covalent catalysis<sup>7</sup>. During the sugar nucleotide metabolism, UGDH

<sup>1</sup>Anorectal Department, Yinchuan Traditional Chinese Medicine Hospital, Ningxia Medical University, Yinchuan 750002, Ningxia Hui Autonomous Region, People's Republic of China. <sup>2</sup>Pathology Department, Yinchuan Traditional Chinese Medicine Hospital, Ningxia Medical University, Yinchuan 750002, Ningxia Hui Autonomous Region, People's Republic of China. <sup>3</sup>Pathology Department, People's Hospital of Ningxia Hui Autonomous Region, Yinchuan 750002, Ningxia Hui Autonomous Region, People's Republic of China. <sup>4</sup>Xiamen Hospital of Traditional Chinese Medicine, Xiamen 361006, People's Republic of China. <sup>5</sup>Key Laboratory of Chinese Internal Medicine of Ministry of Education and Beijing, Dongzhimen Hospital, Beijing University of Chinese Medicine, Beijing 100700, People's Republic of China. <sup>6</sup>Mengyuan Wang and Zhiming Ge contributed equally to this work. <sup>∞</sup>email: A3417@bucm.edu.cn; nxycyy0605@163.com

is a rate-limiting enzyme that participates in the biosynthesis of glycosaminoglycans, including hyaluronan, chondroitin sulfate, and heparan sulfate. Importantly, these glycosylated compounds synthesized under UGDH regulation are prevalent in the extracellular matrix and are likely involved in signal transduction, cell migration, cancer growth, and cancer metastasis. Thus, UGDH has been considered a molecular indicator of tumor progression in multiple cancer types, and an enzyme to be exploited as a potential prognostication marker in oncology and a therapeutic target in cancer biology.

In recent years, researchers have devoted significant attention to the role of UGDH in malignant tumors. UGDH accelerates SNA11 mRNA decay and impairs lung cancer metastasis<sup>11</sup>; UGDH supports autophagy-deficient pancreatic ductal adenocarcinoma growth via increasing hyaluronic acid biosynthesis<sup>12</sup>; UGDH limits prostate androgen availability without impacting hyaluronan levels and is a novel field-specific candidate biomarker of prostate cancer<sup>13,14</sup>; Targeting UGDH inhibits glioblastoma growth and migration<sup>15,16</sup>; UGDH knockout impairs migration and decreases metastatic ability of breast cancer cells, and UGDH is a prognostic marker in breast cancer patients<sup>17,18</sup>; UGDH up-regulation correlated with increased metastatic potential, decreased patient survival, and drug resistance in hepatocellular carcinoma<sup>19,20</sup>; UGDH promotes tumor-initiating cells and a fibroinflammatory tumor microenvironment in ovarian cancer and targeting UGDH inhibits ovarian cancer growth and metastasis<sup>21,22</sup>. Additionally, UGDH is closely associated with tumor drug resistance<sup>23</sup>, epithelial-mesenchymal transition<sup>24</sup>, and cellular localization<sup>25</sup>. The above studies indicate that UGDH has broad and diverse regulatory effects in cancers, and it is also a promising target for diagnosing and treating tumors.

Owing to the aging population and unfavorable risk factors such as obesity, a lack of physical exercise, and smoking, colorectal cancer (CRC) is the third most common and the second deadliest cancer worldwide, and the high mortality rate indicates a lack of success for current treatment methods<sup>26</sup>. Accumulating evidence shows that the abnormal metabolic program provides CRC cells with abundant energy, nutrients, and redox requirements to support their malignant growth and metastasis, which is accompanied by impaired metabolic flexibility in the tumor microenvironment (TME) and dysbiosis of the gut microbiota<sup>27</sup>. However, the role of UDP acid metabolism and the expression, prognostic value, correlated signaling pathways, and impacts on immune cell infiltration of UGDH in CRC have rarely been studied.

Therefore, in this study, we designed bioinformatics analysis, clinical sample testing, and in vitro experiments to detect the expression and analyze the potential role of UGDH in CRC, including its expression characteristics, diagnostic and prognostic value, enrichment analysis, and genetic alterations. We subsequently investigated the role of UGDH in immunotherapy and its potential as a therapeutic target by studying its association with ICIs and immune checkpoint genes. With this study, we expect to clarify the expression of UGDH in CRC, its prognostic value, its relationship with the immune microenvironment, and its regulatory effect and mechanism on CRC cells.

# Methods

#### Data acquisition

We employed TCGA (https://cancergenome.nih.gov) and the GTEx project (https://gtexportal.org/) to obtain comprehensive data on UGDH mRNA expression in tumor samples, corresponding paracancerous tissues, and normal controls. Gene expression profiles of the original datasets were derived from the GEO (https://www.ncbi.nlm.nih.gov/geo/). We filter a sample with an expression level of 0 and then perform a log2 (x+0.001) transformation for each expression value. The protein expression data of UGDH were obtained from the HPA (http://www.proteinatlas.org) and CPTAC (https://proteomics.cancer.gov) databases.

# Clinical samples and patient information

Twelve colorectal cancer (CRC) samples were collected from the Yinchuan Traditional Chinese Medicine Hospital. All samples were histopathologically confirmed with CRC criteria. The clinicopathological characteristics of patients, including gender, age, tumor type, and tumor site, were shown in Supplementary Table S1. The Ethics Committee of Yinchuan Traditional Chinese Medicine Hospital approved the study protocol. During the study, we confirm that the informed consent of all participants and/or their legal guardians has been obtained. Research involving human research participants was conducted following the Declaration of Helsinki.

# **Expression analysis of UGDH**

UGDH expression in normal and tumor tissues was analyzed via the TNMplot (https://tnmplot.com/analysis/)<sup>28</sup>, GEPIA (http://gepia.cancer-pku.cn)<sup>29</sup>, and UALCAN (https://ualcan.path.uab.edu)<sup>30</sup> platforms. The genes correlated with UGDH expression were analyzed via the UALCAN platform.

#### Genomic alteration analysis of UGDH

The copy number variation (CNV) data for UGDH were retrieved from the MEXPRESS database (https://mexpress.ugent.be/)<sup>31</sup>. The methylation levels of the UGDH gene in CRC tissues were analyzed via the UALCAN platform. The single nucleotide variation (SNV) and expression of UGDH were analyzed via the Sangerbox platform (http://sangerbox.com)<sup>32</sup>.

# Diagnostic analysis of UGDH in CRC

The data of CRC patients were downloaded from the TCGA. The diagnostic value of UGDH was assessed via receiver operating characteristic (ROC) curves in CRC. The mRNA expression data of UGDH in malignant and normal tissues from the TCGA database were used to construct these ROC curves. The curves were depicted via the "ggplot2" package (version 3.3.6), and the "pROC" package (version 1.18.0) in R was used to conduct the ROC analysis. The diagnostic metrics that were calculated were the area under the curve (AUC), cutoff values,

sensitivity, specificity, positive predictive value, and negative predictive value. Superior diagnostic accuracy is suggested by an AUC value that is nearly 1. Nomograms and calibrations were employed to evaluate the prognostic significance of clinical characteristics for the prognosis of patients with tumors via the "rms" and "survival" R packages.

#### Survival analysis of UGDH

The survival data of CRC patients were downloaded from the TCGA. The "survival" package (version 3.3.1) in R (version 4.2.1) was used to conduct Kaplan-Meier (K-M) survival analysis. This analysis compared the rates of overall survival (OS), disease-specific survival (DSS), disease-free interval (DFI), and progression-free interval (PFI) between the high and low UGDH gene expression groups. Furthermore, the Kaplan-Meier plotter (KMP) platform (https://www.kmplot.com), which collects data from 16 GEO datasets, was used to assess the survival value of UGDH in CRC patients and autoselects the best cutoff<sup>33</sup>.

# Cancer stage and molecular subtype analysis of UGDH

The "cancer stage" and "molecular subtype" modules of the TISIDB database (http://cis.hku.hk/TISIDB/)<sup>34</sup> were employed to examine the relationships between *UGDH* mRNA expression in CRC.

#### Immune-related characteristics of UGDH

Estimation of the proportions of stromal and immune cells in malignant tumor tissues via expression data (ESTIMATE), Tumor Immune Estimation Resource (TIMER), and Microenvironment Cell Populations-counter (MCPcounter), estimation of the proportion of immune and cancer cells (EPIC), quantification of the tumor immune contexture from human RNA-seq data (quanTIseq), and immunophenoscore (IPS) analyses of *UGDH* expression in CRC were performed via the Sangerbox platform. The "GSVA" package (version 1.44.5) with the ssGSEA algorithm was employed to evaluate the correlation between UGDH expression and tumor-infiltrating lymphocytes, MHC molecules, immunostimulators, immunoinhibitors, chemokines, and chemokine receptors in CRC. Spearman's correlation was employed to determine statistical significance, with p values of less than 0.05 indicating a significant correlation. These correlations were represented as heatmaps via the "ggplot2" package (version 3.3.6).

#### Functional enrichment analysis of UGDH

Gene Ontology (GO) and Kyoto Encyclopedia of Genes and Genomes (KEGG) pathway enrichment analyses are knowledge bases for systematic analysis of gene functions, linking genomic information with higher-order functional information<sup>35–38</sup>. GO and KEGG pathway enrichment analyses of genes were performed via the DAVID database (https://david.ncifcrf.gov/). An FDR<0.1 and a p value<0.05 were set as the significant enrichment cutoff.

# Protein-protein interaction network construction

The UGDH-related genes were input into the STRING platform (https://string-db.org/), with confidence scores set to 0.4 or higher, and restricted to *H. sapiens*, yielding protein-protein interaction (PPI) data, which were then analyzed via Cytoscape 3.10.1 (https://cytoscape.org/).

#### Histology staining analysis

The tissues were fixed overnight in 4% formalin (Servicebio, G1101, CN) and embedded in paraffin. Tissue sections were stained with hematoxylin and eosin (HE) staining using a kit from Servicebio (G1003, CN) to observe the structure. The quantification of the positively stained area was calculated by ImageJ software.

#### Immunohistochemistry (IHC) analysis

For IHC, the tissue sections were deparaffinized and rehydrated before antigen retrieval, removal of endogenous peroxidase, and blocking with normal goat serum. To detect proliferating cells, the Ki67 antibody (mouse mAb, GB121499, Servicebio, CN) was added dropwise with incubated in a wet chamber overnight at 4 °C. To detect UGDH, the paraffin-embedded sections were incubated overnight at 4 °C with the primary anti-UGDH (mouse mAb, Proteintech, 67360-1-Ig, US). The next day, the reaction solution and HRP-labeled anti-mouse secondary antibody (GB23301, Servicebio, CN) were added dropwise and incubated at 37 °C for 30 minutes. Diaminobenzidine (G1212, Servicebio, CN) was applied to provide a chromogen, referring in a reddish-brown color. Positive expression was defined as brown-yellow granules in the cytoplasm.

# Cell culture

NCM460, HT-29, Caco-2, and HCT-8 cell lines were acquired from the American Type Culture Collection (Manassas, VA, USA) and subsequently maintained in Dulbecco's modified Eagle's medium (DMEM) supplemented with 10% fetal bovine serum (FBS), 100 U/mL penicillin, 100 µg/mL streptomycin, and 5% CO<sub>2</sub>.

#### Knockdown of UGDH

HCT-8 cells were seeded at a confluency of 60–80% for lentivirus infection 24 hours prior. Table 1 shows information on the siRNAs targeted to the UGDH gene. The insertion sequence of the control was TTCTC CGAACGTGTCACGT. The lentiviral vector used was GV493. The lentivirus was provided by GeneChem Corporation (Shanghai, China), and the infected cells were further treated with puromycin (10 ng/ml, CSGC32186, Chemstan, China).

| No.          | 5′         | STEM                  | Loop   | STEM                  | 3′     |
|--------------|------------|-----------------------|--------|-----------------------|--------|
| UGDH-RNAi1-a | Ccgg       | CCGAAGTTTAGTCTTCAAGAT | CTCGAG | ATCTTGAAGACTAAACTTCGG | TTTTTg |
| UGDH-RNAi1-b | aattcaaaaa | CCGAAGTTTAGTCTTCAAGAT | CTCGAG | ATCTTGAAGACTAAACTTCGG |        |
| UGDH-RNAi2-a | Ccgg       | GCCATCAAAGAAGCTGATCTT | CTCGAG | AAGATCAGCTTCTTTGATGGC | TTTTTg |
| UGDH-RNAi2-b | aattcaaaaa | GCCATCAAAGAAGCTGATCTT | CTCGAG | AAGATCAGCTTCTTTGATGGC |        |
| UGDH-RNAi3-a | Ccgg       | CGGATCATAGATAGTCTGTTT | CTCGAG | AAACAGACTATCTATGATCCG | TTTTTg |
| UGDH-RNAi3-b | aattcaaaaa | CGGATCATAGATAGTCTGTTT | CTCGAG | AAACAGACTATCTATGATCCG |        |

**Table 1**. The SiRNA sequence.

| Gene           | Sequence                |  |  |  |
|----------------|-------------------------|--|--|--|
| UGDH           |                         |  |  |  |
| Forward Primer | CCCTGTGTGCTGTATATGAGC   |  |  |  |
| Reverse Primer | TGCTTATTCTCTGGGCAAGAAAA |  |  |  |
| GAPDH          |                         |  |  |  |
| Forward Primer | GGAGCGAGATCCCTCCAAAAT   |  |  |  |
| Reverse Primer | GGCTGTTGTCATACTTCTCATGG |  |  |  |

**Table 2**. The qRT-PCR primers.

#### Cell viability assay

A total of  $5 \times 10^3$  cells were inoculated in 96-well plates for 24, 48, or 72 hours. To evaluate the capacity for cell proliferation, the absorbance at 450 nm was measured via a TECAN Infinite M200 Multimode microplate reader (Tecan, Mechelen, Belgium) with a CCK-8 assay kit (Solarbio, CN). The experiments were performed in six replicates and were repeated 3 times.

#### Wound healing assay

A total of  $5\times10^5$  cells were seeded in a 12-well plate. Twelve hours later, the cell monolayer was scratched with a sterile 10- $\mu$ L pipette tip to generate a line-shaped wound. The cells were subsequently cultured in DMEM without FBS. After 48 hours, images of the scratches were acquired with a digital camera. The scratch areas were quantified via Image Pro-Plus 6.0 software (Media Cybernetics Inc., US). The experiments were performed in triplicate and repeated 3 times.

#### Quantitative real-time polymerase chain reaction (qRT-PCR)

Total RNA was extracted, and cDNA was synthesized via an EasyScript\* All-in-One First-Strand cDNA Synthesis SuperMix Kit (Transgene, Beijing, China). Relative quantification was conducted in triplicate via real-time PCR on a QuantStudio 6 Pro Real-Time PCR System (Thermo Fisher Scientific, Waltham, US) with TransStart\* Top Green qPCR SuperMix (Transgene, Beijing, China). We employed GAPDH as an internal control gene. The experiments were conducted in triplicate and repeated three times. Table 2 lists the primers used in this investigation.

#### Western blot

The protein lysates were separated via 10% sodium dodecyl sulfate-polyacrylamide gel electrophoresis (SDS-PAGE) (Epizyme Biomedical Technology, PG112, CN) and subsequently electrophoretically transferred onto polyvinylidene fluoride membranes (Epizyme Biomedical Technology, WJ001, CN). Anti-UGDH (Proteintech, 67360-1-Ig, 1:1000, US) and anti-GAPDH (MBL, M171-3, 1:5000, JPN) primary antibodies were used. The secondary antibody used was HRP-conjugated AffiniPure goat anti-mouse IgG (H+L) (Proteintech, SA00001-1, 1:8000, US). The integrated density of the protein bands was analyzed via ImageJ software.

# Statistical analysis

The data are presented as the means ± standard deviations (SDs). Statistical significance was assessed via Student's t test or the Mann–Whitney test for comparisons between two groups. One-way analysis of variance (ANOVA) followed by appropriate post hoc tests was employed when more than two groups were compared. All the statistical analyses were performed via SPSS 25.0 software (IBM Co., NY, USA). Group differences were deemed statistically significant if the *P* value was less than 0.05.

# Results

#### **Expression of UGDH in CRC**

In the TCGA and TNM plot databases, *UGDH* mRNA expression levels were significantly lower in CRC tissues than in normal tissues (Fig. 1A&B). In GEO datasets, including GSE74602, GSE10950, and GSE110224, the results also demonstrated the downregulation of *UGDH* mRNA in CRC (Figure S1A). Furthermore, in the TNM plot database, metastatic CRC tissues presented significantly lower expression levels than nonmetastatic

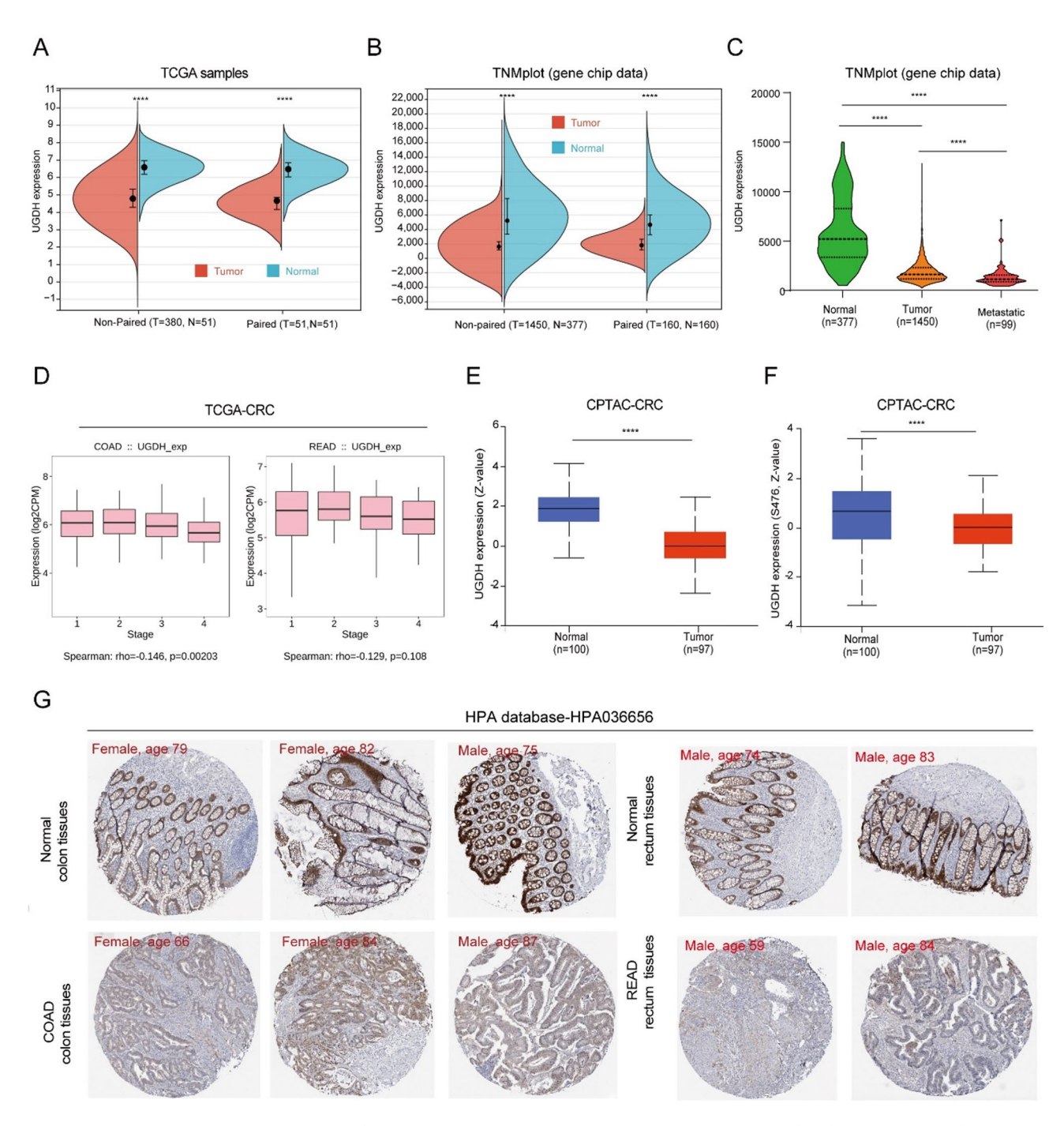


**Fig. 1.** Expression of UGDH in CRC. **(A)** *UGDH* mRNA expression in normal and CRC tissues in the TCGA database. **(B)** The *UGDH* mRNA expression of normal and CRC tissues in the TNMplot database. **(C)** *UGDH* mRNA expression in normal, nonmetastatic, and metastatic CRC tissues in the TNM plot database. **(D)** *UGDH* mRNA expression in CRC tissues from different tumor stage groups. **(E)** Total UGDH protein expression in normal and CRC tissues in the TCGA database. **(F)** Phosphorylated UGDH protein expression in normal and CRC tissues in the TCGA database. **(G)** UGDH protein expression in normal and CRC tissues in the TCGA database. **(G)** UGDH protein expression in normal and CRC tissues in the HPA database. \*\*\*\*\*p < 0.0001.

CRC tissues did (Fig. 1C). In COAD tissues, *UGDH* mRNA expression decreases with increasing tumor stage (Fig. 1D). The CPTAC data revealed that the total protein and phosphoprotein levels of UGDH were lower in CRC tissues than in normal tissues (Fig. 1E&F). Immunohistochemical staining of clinical samples from the HPA database also revealed downregulation of the UGDH protein in CRC tissues compared with normal tissues (Fig. 1G). We further detected the UGDH expression of clinical CRC samples, and the result showed that the UGDH protein was downregulated in tumor tissues compared with non-tumor tissues in the same sample (Fig. 2).

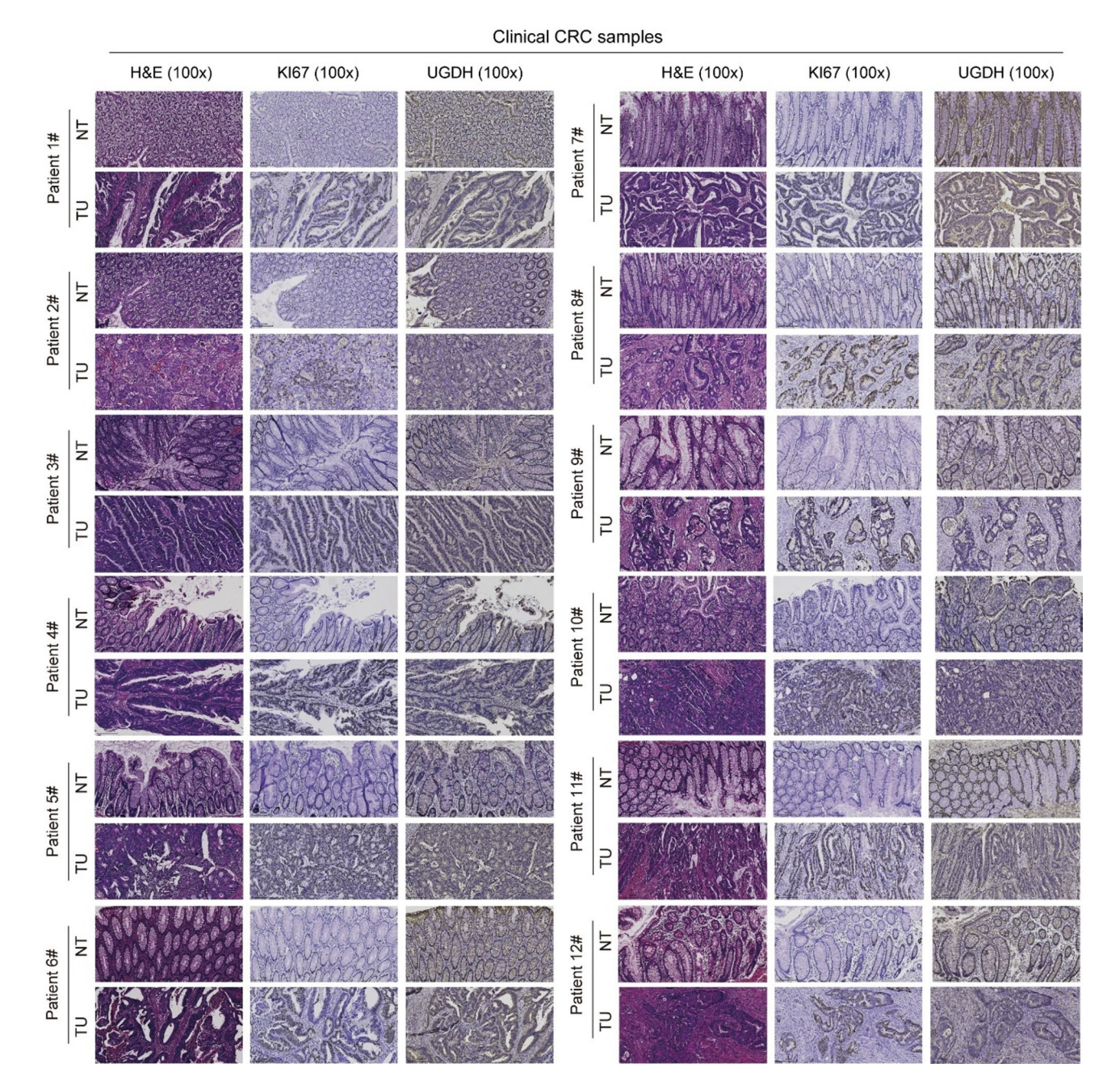


Fig. 2. H&E staining and IHC staining of KI67 and UGDH of clinical CRC samples.

# Prognostic value of UGDH in CRC

The diagnostic utility of UGDH mRNA expression was assessed for normal and CRC tissues via receiver operating characteristic (ROC) curve analysis, and the results revealed that *UGDH* had high diagnostic value (Fig. 3A). The Kaplan-Meier plotter survival analysis suggested that high UGDH expression was significantly related to good overall survival (OS), RFS, and PFS in CRC patients (Fig. 3B-D). In the TCGA-CRC database, the results also revealed that high UGDH expression was related to good OS, DSS, DFI, and PFI in CRC patients (Supplemental Figure S2). To obtain a better model for predicting survival in CRC patients than individual prognostic factors, we constructed a nomogram model based on UGDH expression in combination with multiple clinical prognostic factors, including the age at initial diagnosis, sex, and tumor stage (Fig. 3E). The calibration curve (C-index = 0.72, Fig. 3F) and K-M plot of the risk score also revealed the good predictive ability of the nomogram model for CRC (Fig. 3G).

# Genetic alterations of UGDH in CRC

Compared with that in normal tissues, the methylation level of the *UGDH* gene promoter in tumor tissues was significantly greater (Fig. 4A) and was significantly negatively correlated with *UGDH* mRNA expression (Fig. 4B). In CRC tumor tissues, the main gene copy number variation (CNV) type of the *UGDH* gene was

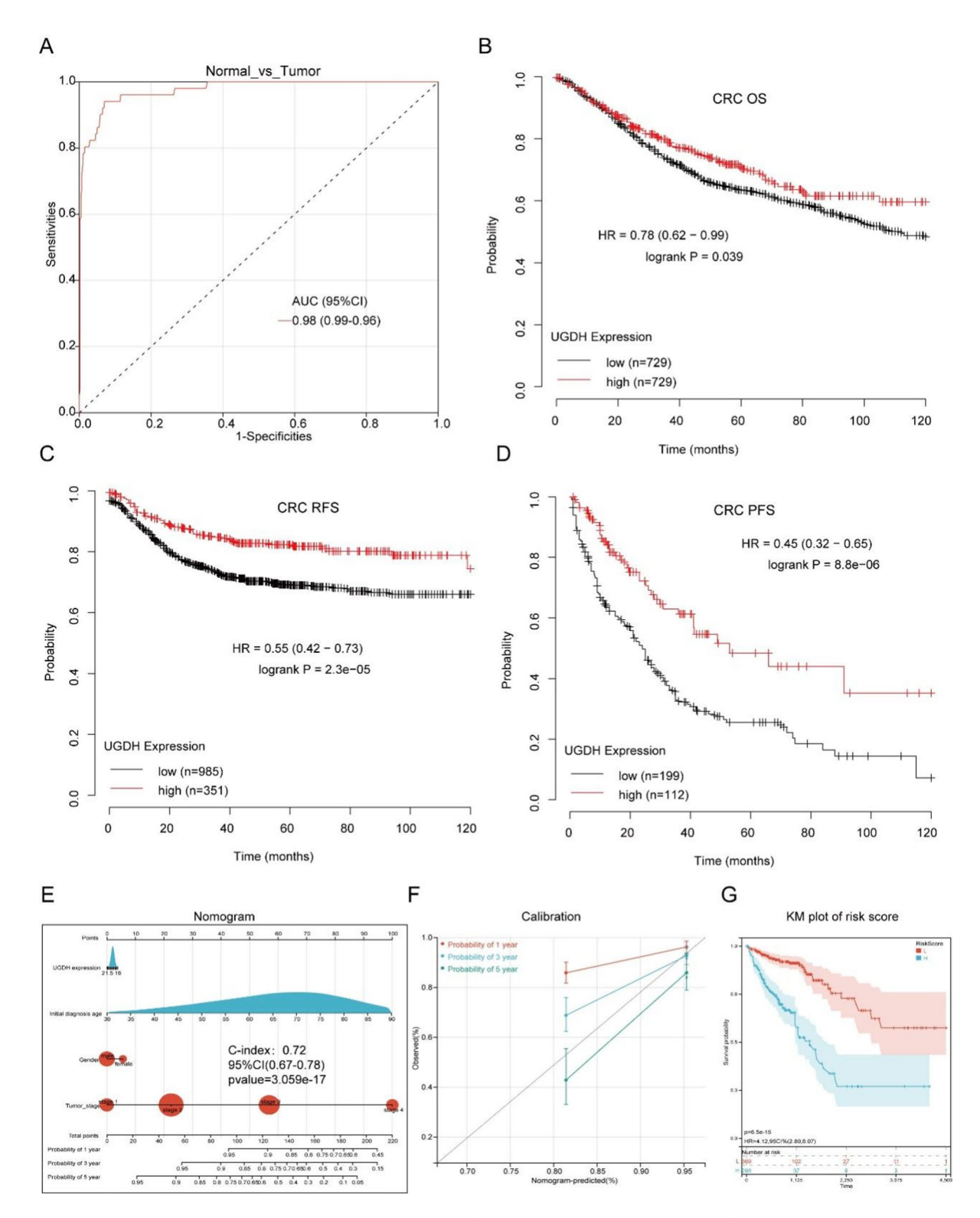


**Fig. 3.** The diagnostic and prognostic value of UGDH in CRC. (**A**) ROC curve of *UGDH* mRNA expression in CRC. (**B**) OS analysis between *UGDH* mRNA expression and CRC. (**C**) RFS analysis between *UGDH* mRNA expression and CRC. (**D**) PFS analysis between *UGDH* mRNA expression and CRC. (**E**) A nomogram that combines *UGDH* mRNA expression and other prognostic factors in CRC. (**F**) Calibration curve of the nomogram. (**G**) KM plot analysis of the risk factors for the nomogram in CRC.

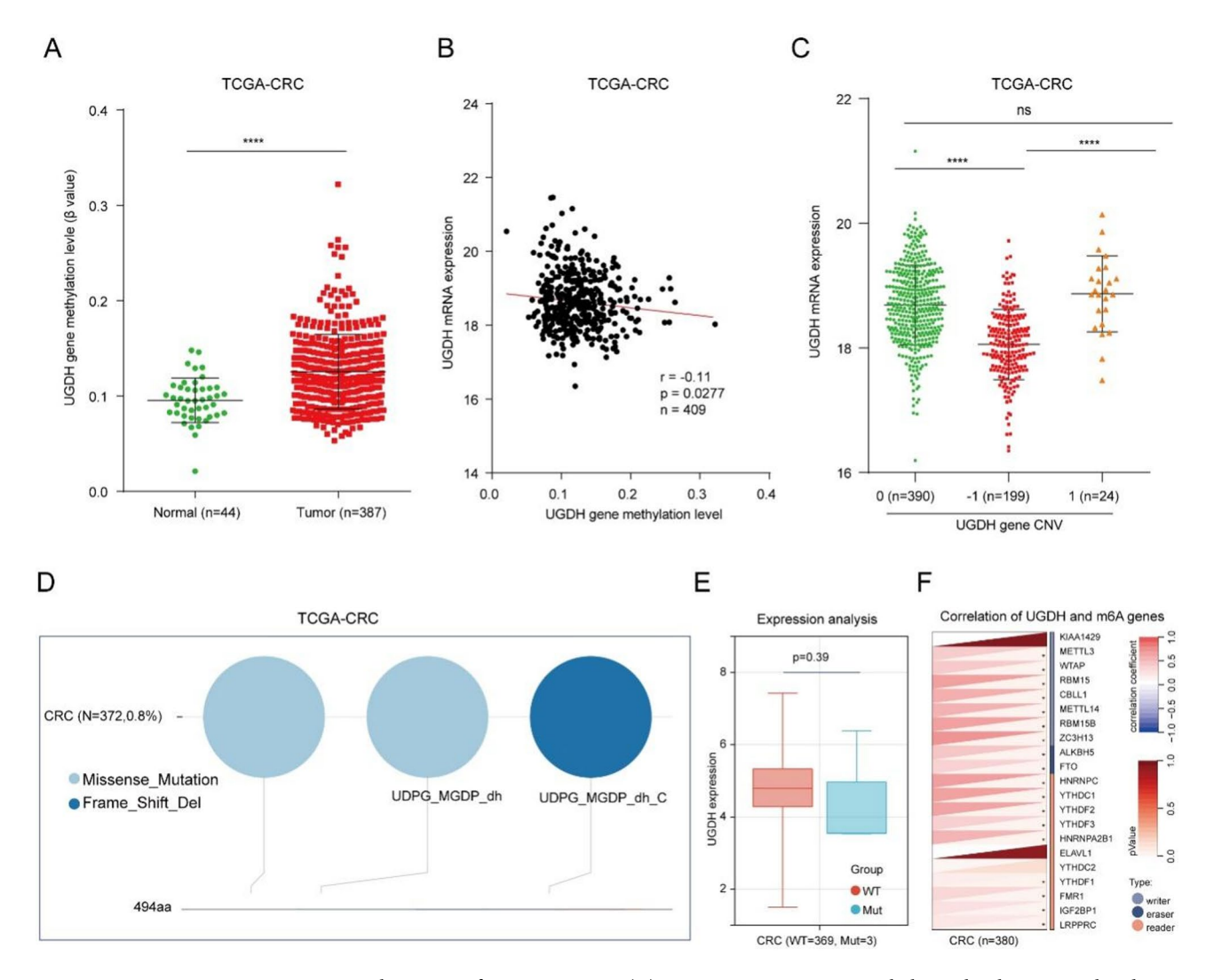


**Fig. 4.** Genetic alterations of UGDH in CRC. (**A**) *UGDH* gene promoter methylation levels in normal and CRC tissues. (**B**) Correlation analysis between the *UGDH* gene promoter methylation level and *UGDH* mRNA expression in CRC. (**C**) *UGDH* mRNA expression in tumor tissues from the neutral, deletion, and duplication groups in the TCGA-CRC database. (**D**) Information on *UGDH* gene mutations in CRC. (**E**) *UGDH* mRNA expression in WT and mutant CRC tissues. (**F**) mRNA expression correlations between *UGDH* and m6A-related genes in CRC. \*\*\*\*p<0.001; \*\*\*\*\*p<0.0001. ns not significant.

deletion (-1, 32.3%), and compared with that in the CNV normal (0) group, *UGDH* mRNA expression was significantly downregulated in the CNV deletion group (Fig. 4C). Furthermore, the mutational landscape of the *UGDH* gene in CRC was further explored. We found that 3 (0.8%) of the 372 CRC samples had UGDH gene mutations (Fig. 4D). There was no significant difference in *UGDH* expression between the wild-type and mutant UGDH samples. (Fig. 4E). The correlation analysis results revealed that *UGDH* mRNA was positively correlated with most m6A-related genes (Fig. 4F).

# Correlations between UGDH and the TP53 pathway in CRC

The TP53 tumor suppressor gene is the most frequently altered gene in human cancers and has been a major focus of oncology research<sup>39</sup>. Herein, we further explored the correlation between UGDH and the TP53 pathway in CRC. First, compared with that in TP53-nonmutant CRC tissues, *UGDH* mRNA expression was significantly lower in *TP53*-mutant CRC tissues (Fig. 5A), which presented a lower methylation level (Fig. 5B). At the protein level, UGDH expression also tended to decrease in p53/Rb-related pathway-altered CRC tissues (Fig. 5C&D). Furthermore, there was a significant positive correlation between *UGDH* and *TP53* expression in both tumor and normal colon tissues (Fig. 5E&F). Overall survival analysis of CRC patients revealed that high UGDH mRNA expression was associated with a better prognosis in the wild-type *TP53* group than in the mutated *TP53* group (Fig. 5G).

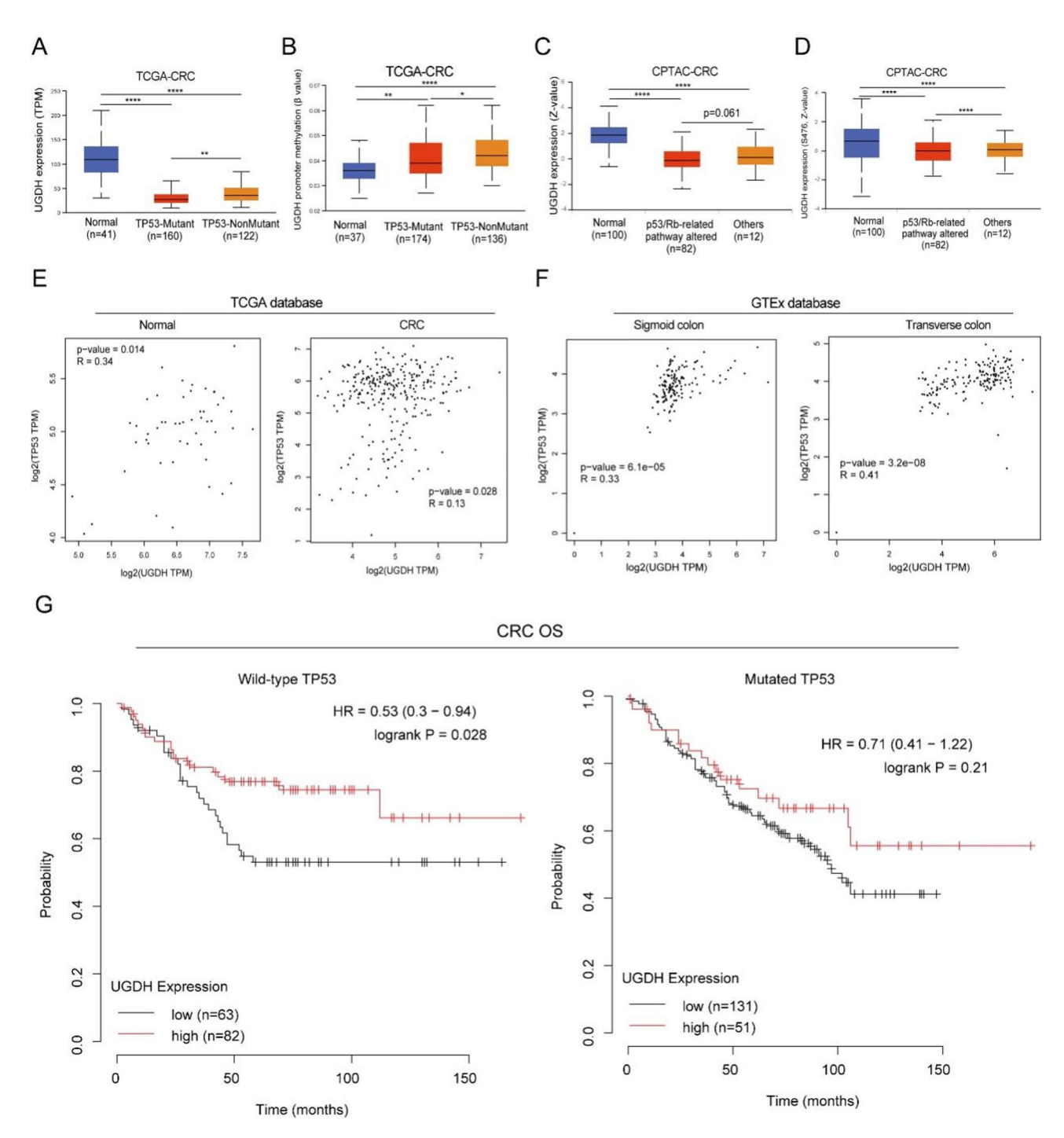
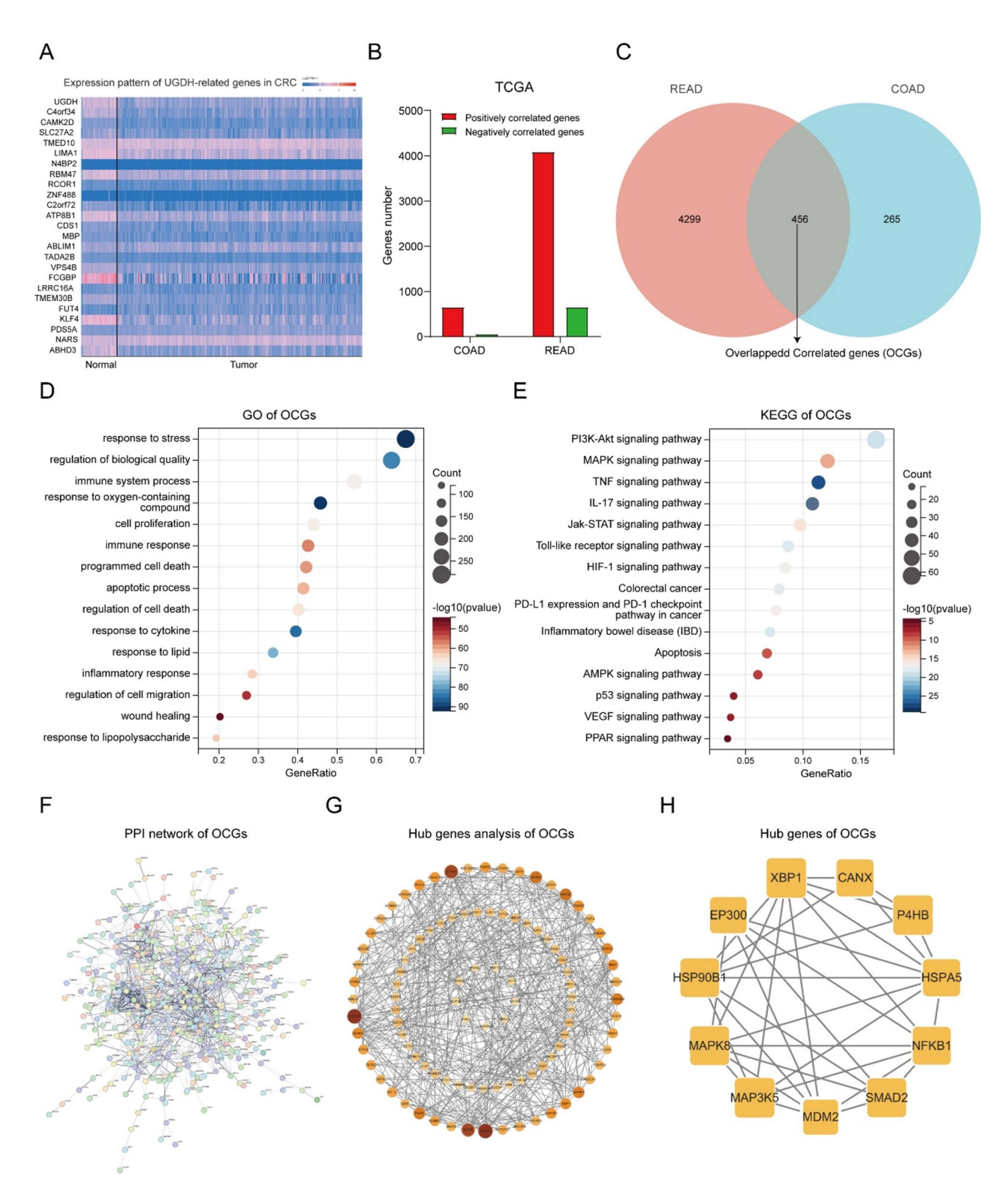


Fig. 5. Correlation of UGDH and the TP53 pathway in CRC. (A) UGDH mRNA expression in normal, TP53-Mutant CRC, and TP53-NonMutant CRC tissues. (B) UGDH gene promoter methylation levels in normal, TP53-Mutant CRC, and TP53-NonMutant CRC tissues. (C) UGDH total protein expression in normal, TP53-Mutant CRC, and TP53-NonMutant CRC tissues. (D) Phosphorylated UGDH protein expression in normal, TP53-Mutant CRC, and TP53-NonMutant CRC tissues. (E) mRNA expression correlation of UGDH and UGDH mRNA expression and CRC in the wild-type UGDH and UGDH mutant UGDH mRNA expression and CRC in the wild-type UGDH mutant UGDH mutant UGDH mutant UGDH mrnA expression and CRC in the wild-type UGDH mutant UGDH mutant UGDH mrnA expression and CRC in the wild-type UGDH mutant UGDH mutant UGDH mrnA expression and UGDH mutant UGDH mutant UGDH mutant UGDH mrnA expression and UGDH mutant UGDH

# Functional enrichment analysis of UGDH-related genes in CRC

We analyzed the genes related to UGDH expression in CRC (Fig. 6A&B). A total of 456 overlapping correlated genes (OCGs) were obtained between the two groups (Fig. 6C), and detailed information on the correlated genes is provided in Supplement Table S2. The GO enrichment analysis revealed that these OCGs were enriched mainly in immune system process, cell proliferation, programmed cell death, regulation of cell migration, and



**Fig. 6.** Enrichment analysis of UGDH expression-related genes. (**A**) Expression heatmap of UGDH expression-related genes in normal and CRC tissues. (**B**) Number of UGDH expression-related genes in COAD and READ. (**C**) Venn analysis of UGDH expression-related genes in COAD and READ. (**D**) GO enrichment analysis of OCGs. (**E**) KEGG enrichment analysis of OCGs. (**F**) The PPI network of OCGs. (**G**) MCODE analysis of OCGs via Cytoscape. (**H**) Hub genes of OCGs.

response to lipopolysaccharide (Fig. 6D). The KEGG enrichment analysis indicated that these OCGs were related primarily to the PI3K-Akt signaling pathway, the MAPK signaling pathway, colorectal cancer, apoptosis, the AMPK signaling pathway, the p53 signaling pathway, the VEGF signaling pathway, and the PPAR signaling pathway (Fig. 6E). The detailed information on the enrichment analysis is provided in Supplement Tables S3 and S4. We subsequently constructed a PPI network of the OCGs (Fig. 6F). Using the Cytoscape MCODE component (Fig. 6G), we ultimately obtained 11 hub genes, including CANX, P4HB, HSPA5, NFKB1, SMAD2, MDM2, MAP3K5, MAPK8, HSP90B1, EP300, and XBP1 (Fig. 6H).

# UGDH regulates immune cell infiltration (ICI) in CRC

ESTIMATE analysis revealed a positive correlation between *UGDH* expression and stromal, immune, and Estimate Scores (Fig. 7A). The IPS analysis results indicated that *UGDH* expression was positively correlated with the MHC and EC scores and negatively correlated with the SC, CP, and AZ scores (Fig. 7B). QuanTlseq analysis revealed positive correlations between *UGDH* expression and M1 and M2 macrophages, neutrophils, NK cells, CD8+T cells, and Tregs (Fig. 7C). EPIC analysis revealed that *UGDH* expression was positively correlated with CAFs, endothelial cells, and macrophages (Fig. 7D). TIMER analysis revealed that B cells, CD4+T cells, CD8+T cells, neutrophil cells, macrophages, and dendritic cells (DCs) were positively correlated with *UGDH* expression (Fig. 7E). According to the MCPcounter analysis, *UGDH* expression was positively correlated with T cells, cytotoxic lymphocytes, NK cells, monocytic lineage cells, DCs, neutrophil cells, endothelial cells, and fibroblasts (Fig. 7F). Because immunomodulators and immune checkpoints strongly impact the immunological microenvironment, we further investigated the relationship between *UGDH* and immunomodulators and immune checkpoints in CRC. The results suggested that UGDH is positively related to most immunomodulators in CRC (Figure S2).

#### UGDH downregulation promotes the proliferation and migration of CRC cells

We first examined the endogenous protein expression levels of UGDH in NCM460, HT-29, Caco-2, and HCT-8 cell lines. The HCT-8 cell line showed the highest expression level and was used for further experiments (Fig. 8A). We performed siRNA lentivirus infection in HCT-8 cells to knock down the expression of UGDH (Fig. 8B). qRT-PCR and Western blotting analysis demonstrated that the UGDH expression level was substantially reduced in HCT-8 cells (Fig. 8C&D). The proliferative activity of HCT-8 cells was markedly enhanced by the knockdown of UGDH at 72 h, as demonstrated by the CCK-8 analysis (Fig. 8E). The scratch assay results demonstrated that UGDH downregulation promoted the migration ability of HCT-8 cells (Fig. 8F).

#### Discussion

Studies have shown that downregulation of UGDH affects glycosaminoglycan synthesis and motility in HCT-8 cells<sup>40</sup> and has been identified as a differentially expressed gene in clinical CRC samples associated with metabolism-related functions<sup>41</sup>. However, the expression status and function of UGDH in CRC are unclear.

In our study, we first confirmed the downregulation of UGDH in clinical CRC tissues compared with normal tissues. At the genome level, aberrant DNA methylation is an essential epigenetic regulator of gene expression and genome stability that drives tumor progression<sup>42</sup>. Our results revealed that, compared with those in normal samples, the methylation levels of the *UGDH* gene promoter are significantly increased, which indicates that increased methylation of the *UGDH* gene promoter could inhibit *UGDH* mRNA expression. On the other hand, CNVs of the genome can also impact gene expression, which has been linked to complex traits in humans, including disease and drug response<sup>43</sup>. Our results revealed that in CRC tissues, the main CNV type of the UGDH gene is deletion, which is correlated with lower *UGDH* mRNA expression. At the mRNA level, m6A methylation is the most abundant modification in mRNAs and plays an important role in the metabolic reprogramming of tumor cells<sup>44</sup>. Our results revealed positive correlations between *UGDH* mRNA expression and most m6A-related genes. These results highlight the multiple regulatory mechanisms of UGDH expression in CRC, and the detailed mechanism needs further study at the molecular level.

We next analyzed the relationship between UGDH and the tumor microenvironment, which is essential for tumorigenesis, development, metastasis, and therapeutic response, and the infiltration and activation status of immune cells can strongly influence their function<sup>45</sup>. It has been reported that downregulating UGDH in glioblastoma cells can activate human primary macrophages and promote human T-cell migration, proliferation, and activation<sup>16</sup>. Our GO enrichment analysis revealed that UGDH and its correlated genes are involved in immune and inflammatory responses. The ICI analysis further demonstrated the correlations between *UGDH* mRNA expression and immune status in CRC. The application of immune checkpoint inhibitor-based immunotherapy in CRC has yielded satisfactory results in terms of safety and efficacy<sup>46</sup>. Thus, targeting UGDH to regulate the immune status and improve immunotherapy efficacy might be an avenue of great potential. However, more experiments and clinical trials are needed to confirm these findings.

Finally, we further performed in vitro experiments and confirmed that downregulating UGDH promoted the proliferation and migration of CRC cells. Thus, we believe that UGDH is a tumor suppressor gene in CRC. Interestingly, we found that *UGDH* expression was positively correlated with the *TP53* expression, and significantly different between *TP53*-Mutant and *TP53*-NonMutant CRC tissues. In the *TP53*-Mutant CRC group, *UGDH* expression significantly correlated with prognosis, while it had no significant correlation in the *TP53*-NonMutant group. Our KEGG analysis also revealed that UGDH and its correlated genes are enriched in the apoptosis and p53 signaling pathways. Usually, p53 functions as a suppressor of carcinogenesis by regulating genes involved in plasticity, autophagy, the cell cycle, apoptosis, and DNA repair, and there is a link between p53 and apoptosis in CRC<sup>47</sup>. Combining these results, we speculate that UGDH upregulates the expression of p53 and further exerts anti-tumor function in CRC. Nonetheless, the relationship and detailed regulatory

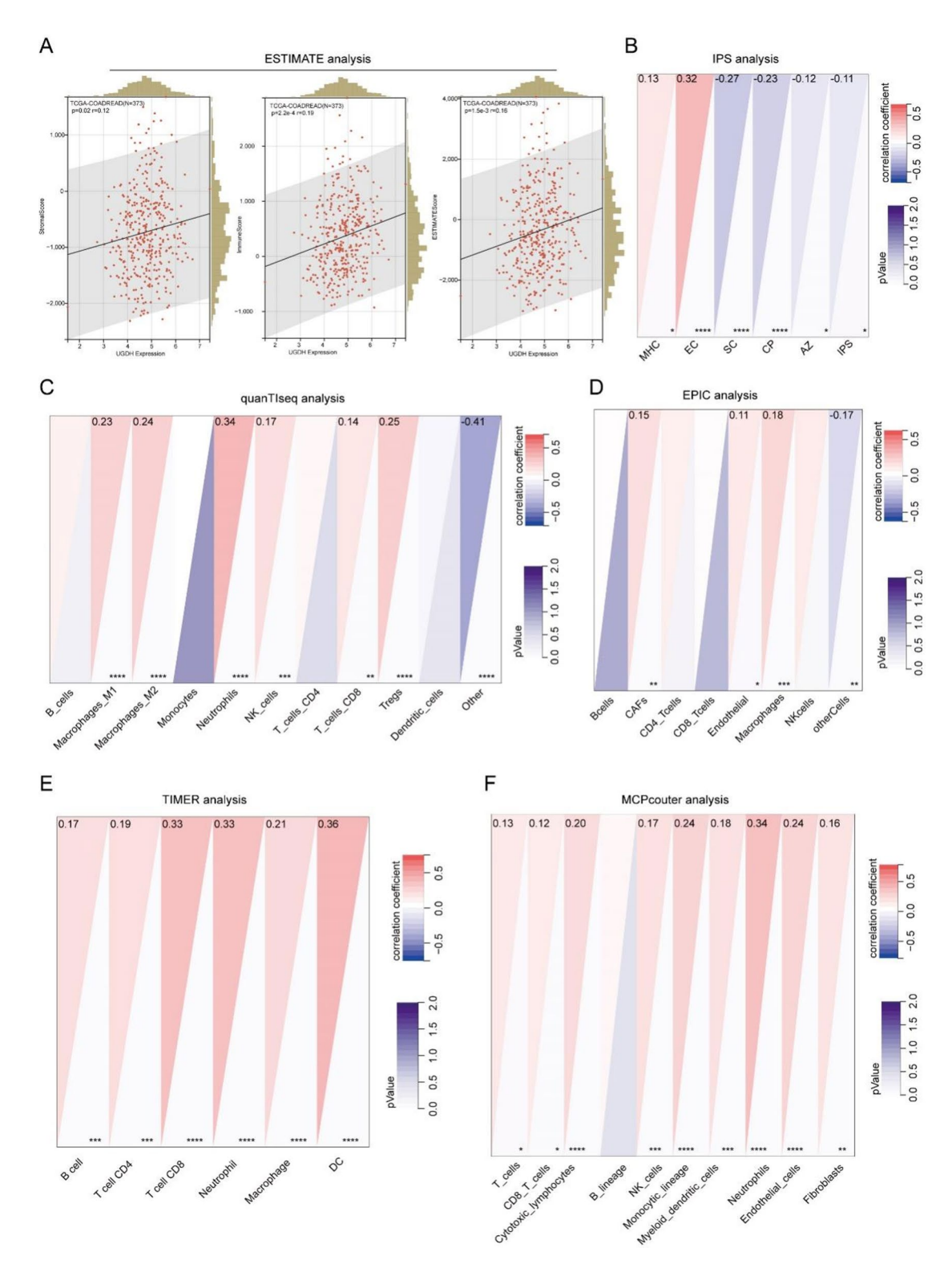


**Fig.** 7. UGDH expression is correlated with immune cell infiltration. (**A**) Estimate analysis of UGDH in CRC; (**B**) IPS analysis of UGDH in CRC; (**C**) QuanTIseq analysis of UGDH in CRC; (**D**) EPIC analysis of UGDH in CRC; (**E**) TIMER analysis of UGDH in CRC; (**F**) MCPcounter analysis of UGDH in CRC. \*p<0.05; \*\*p<0.01; \*\*\*p<0.001; \*\*\*\*p<0.0001.

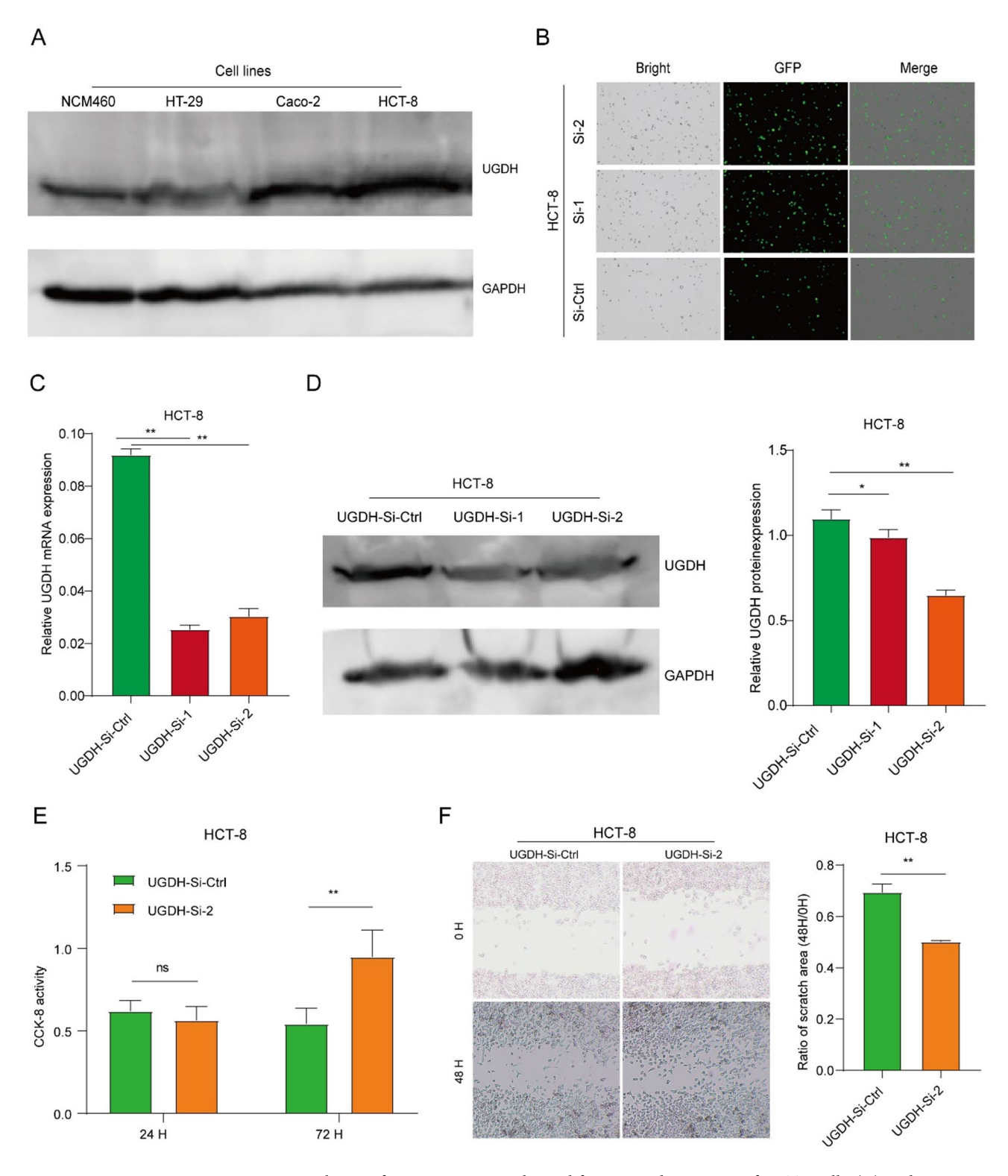


**Fig. 8.** Downregulation of UGDH promotes the proliferation and migration of HCT-8 cells. **(A)** Endogenous UGDH protein expression in colon cell lines; **(B)** The bright field and fluorescence imaging of HCT-8 cells; **(C)** UGDH mRNA expression of Si-control and Si-UGDH HCT-8 cells; **(D)** UGDH protein expression of Si-control and Si-UGDH HCT-8 cells; **(E)** Cell viability assay of HCT-8 cells with or without UGDH knocked down for 24 and 72 h; **(F)** Representative images of wound healing experiments in HCT-8 cells with or without UGDH knocked down for 48 h. \*P<0.05; \*P<0.01; ns, not significant.

mechanism between UGDH and the p53 signaling pathway need further exploration via in vivo and in vitro experiments.

#### Conclusions

UGDH is downregulated in CRC tissues and can potentially serve as a prognostic indicator for CRC. UGDH downregulation promotes the proliferation and migration of CRC cells, which might correlate with the p53 signaling pathway.

# Data availability

The datasets generated and/or analyzed during the current study are available in the Mendeley Data repository (Zao, Xiaobin (2025), "CRC-UGDH", Mendeley Data, V1, https://data.mendeley.com/datasets/dgzkyjrr7y/1, doi: 10.17632/dgzkyjrr7y.1).

Received: 25 February 2025; Accepted: 18 June 2025

Published online: 01 July 2025

#### References

- 1. Zhou, M. et al. Mortality, morbidity, and risk factors in China and its provinces, 1990-2017: a systematic analysis for the global burden of disease study 2017. Lancet 394 (10204), 1145-1158 (2019).
- 2. Hanahan, D. & Weinberg, R. A. Hallmarks of cancer: the next generation. Cell 144 (5), 646-674 (2011).
- 3. Lane, A. N., Higashi, R. M. & Fan, T. W. Metabolic reprogramming in tumors: contributions of the tumor microenvironment. Genes Dis. 7 (2), 185-198 (2020).
- 4. Park, J. H., Pyun, W. Y. & Park, H. W. Cancer metabolism: phenotype, signaling and therapeutic targets. Cells, 9(10). (2020).
- 5. Doshi, M. B. et al. Disruption of sugar nucleotide clearance is a therapeutic vulnerability of cancer cells. Nature 623 (7987), 625-632 (2023).
- 6. Zimmer, B. M., Barycki, J. J. & Simpson, M. A. Integration of sugar metabolism and proteoglycan synthesis by UDP-glucose dehydrogenase. J. Histochem. Cytochem. 69 (1), 13-23 (2021).
- 7. Egger, S. et al. UDP-glucose dehydrogenase: structure and function of a potential drug target. Biochem. Soc. Trans. 38 (5), 1378-1385 (2010)
- 8. Chen, J. & Yang, S. Catalytic mechanism of UDP-glucose dehydrogenase. Biochem. Soc. Trans. 47 (3), 945-955 (2019).
- 9. Pourakbari, R. et al. Implications for glycosylated compounds and their anti-cancer effects. Int. J. Biol. Macromol. 163, 1323-1332
- 10. Price, M. J. et al. UDP-glucose dehydrogenase (UGDH) in clinical oncology and cancer biology. Oncotarget 14, 843-857 (2023).
- 11. Wang, X. et al. UDP-glucose accelerates SNAI1 mRNA decay and impairs lung cancer metastasis. Nature 571 (7763), 127-131 (2019).
- 12. Fan, M. et al. UDP-glucose dehydrogenase supports autophagy-deficient PDAC growth via increasing hyaluronic acid biosynthesis. Cell. Rep. 43 (2), 113808 (2024).
- 13. Huang, D. et al. Udp-glucose dehydrogenase as a novel field-specific candidate biomarker of prostate cancer. Int. J. Cancer. 126 (2), 315-327 (2010).
- 14. Wei, Q. et al. Androgen-stimulated UDP-glucose dehydrogenase expression limits prostate androgen availability without impacting hyaluronan levels. Cancer Res. 69 (6), 2332-2339 (2009).
- 15. Oyinlade, O. et al. Targeting UDP-α-D-glucose 6-dehydrogenase inhibits glioblastoma growth and migration. Oncogene 37 (20), 2615-2629 (2018).
- 16. Zhan, D. et al. Targeting UDP-α-d-glucose 6-dehydrogenase alters the CNS tumor immune microenvironment and inhibits glioblastoma growth. Genes Dis. 9 (3), 717-730 (2022).
- 17. Teoh, S. T., Ogrodzinski, M. P. & Lunt, S. Y. UDP-glucose 6-dehydrogenase knockout impairs migration and decreases in vivo metastatic ability of breast cancer cells. Cancer Lett. 492, 21-30 (2020).
- 18. Vitale, D. L. et al. Initial identification of UDP-Glucose dehydrogenase as a prognostic marker in breast Cancer patients, which facilitates epirubicin resistance and regulates hyaluronan synthesis in MDA-MB-231 cells. Biomolecules, 11(2). (2021).
- 19. Gao, Q. et al. Dysregulated glucuronic acid metabolism exacerbates hepatocellular carcinoma progression and metastasis through the TGF $\beta$  signalling pathway. Clin. Transl Med. 12 (8), e995 (2022).
- 20. Guo, B. et al. UDP-glucose 6-dehydrogenase lessens Sorafenib sensitivity via modulating unfolded protein response. Biochem. Biophys. Res. Commun. 613, 207-213 (2022).
- 21. Harrington, B. S. et al. UGDH promotes tumor-initiating cells and a fibroinflammatory tumor microenvironment in ovarian cancer. J. Exp. Clin. Cancer Res. 42 (1), 270 (2023).
- 22. Lin, L. H. et al. Targeting UDP-glucose dehydrogenase inhibits ovarian cancer growth and metastasis. J. Cell. Mol. Med. 24 (20), 11883-11902 (2020).
- 23. Zhang, X. et al. E3 ligase HERC5-catalyzed UGDH isgylation promotes SNAI1-mediated tumor metastasis and cisplatin resistance in oral squamous cell carcinoma. Biol. Direct. 20 (1), 27 (2025).
- 24. Wang, Q. et al. UDP-glucose dehydrogenase expression is upregulated following EMT and differentially affects intracellular Glycerophosphocholine and acetylaspartate levels in breast mesenchymal cell lines. Mol. Oncol. 16 (9), 1816–1840 (2022)
- 25. Hagiuda, D. et al. Clinicopathological and prognostic significance of nuclear UGDH localization in lung adenocarcinoma. Biomed. Res. 40 (1), 17-27 (2019).
- 26. Abedizadeh, R. et al. Colorectal cancer: a comprehensive review of carcinogenesis, diagnosis, and novel strategies for classified treatments. Cancer Metastasis Rev. 43 (2), 729-753 (2024).
- 27. Nenkov, M. et al. Metabolic reprogramming of colorectal Cancer cells and the microenvironment: implication for therapy. Int. J. Mol. Sci., 22(12). (2021).
- 28. Bartha, Á. & Győrffy, B. TNMplot.com: A web tool for the comparison of gene expression in normal, tumor and metastatic tissues. Int. J. Mol. Sci., 22(5). (2021).
- 29. Tang, Z. et al. GEPIA: a web server for cancer and normal gene expression profiling and interactive analyses. Nucleic Acids Res. 45 (W1), W98-w102 (2017).
- 30. Chandrashekar, D. S. et al. UALCAN: an update to the integrated cancer data analysis platform. Neoplasia 25, 18-27 (2022).
- 31. Koch, A. et al. MEXPRESS: visualizing expression, DNA methylation and clinical TCGA data. BMC Genom. 16 (1), 636 (2015). 32. Shen, W. et al. Sangerbox: A comprehensive, interaction-friendly clinical bioinformatics analysis platform. iMeta 1 (3), e36 (2022).
- Győrffy, B. Integrated analysis of public datasets for the discovery and validation of survival-associated genes in solid tumors. Innov. (Camb). 5 (3), 100625 (2024).
- 34. Ru, B. et al. TISIDB: an integrated repository portal for tumor-immune system interactions. Bioinformatics 35 (20), 4200-4202 (2019).

- 35. Kanehisa, M. & Goto, S. KEGG: Kyoto encyclopedia of genes and genomes. Nucleic Acids Res. 28 (1), 27-30 (2000).
- 36. Kanehisa, M. Toward Understanding the origin and evolution of cellular organisms. Protein Sci. 28 (11), 1947-1951 (2019).
- 37. Kanehisa, M. et al. KEGG for taxonomy-based analysis of pathways and genomes. Nucleic Acids Res. 51 (D1), D587-d592 (2023).
- 38. Gene Ontology Consortium Going forward. Nucleic Acids Res. 43 (Database issue), D1049-D1056 (2015).
- 39. Wang, H. et al. Targeting p53 pathways: mechanisms, structures, and advances in therapy. Signal. Transduct. Target. Ther. 8 (1), 92 (2023).
- 40. Wang, T. P. et al. Down-regulation of UDP-glucose dehydrogenase affects glycosaminoglycans synthesis and motility in HCT-8 colorectal carcinoma cells. *Exp. Cell Res.* **316** (17), 2893–2902 (2010).
- 41. Shen, X. et al. Microarray analysis of differentially-expressed genes and linker genes associated with the molecular mechanism of colorectal cancer. Oncol. Lett. 12 (5), 3250–3258 (2016).
- 42. Nishiyama, A. & Nakanishi, M. Navigating the DNA methylation landscape of cancer. Trends Genet. 37 (11), 1012-1027 (2021).
- 43. Gamazon, E. R. & Stranger, B. E. The impact of human copy number variation on gene expression. *Brief. Funct. Genomics.* **14** (5), 352–357 (2015).
- 44. An, Y. & Duan, H. The role of m6A RNA methylation in cancer metabolism. Mol. Cancer. 21 (1), 14 (2022).
- 45. Fu, T. et al. Spatial architecture of the immune microenvironment orchestrates tumor immunity and therapeutic response. J. Hematol. Oncol. 14 (1), 98 (2021).
- 46. Zhao, W. et al. Colorectal cancer immunotherapy-Recent progress and future directions. Cancer Lett. 545, 215816 (2022).
- 47. Brockmueller, A. et al. Resveratrol and p53: how are they involved in CRC plasticity and apoptosis? J. Adv. Res. 66, 181–195 (2024).

# **Author contributions**

M.W.: Experiments, Data curation, Investigation, Writing. Z.G.: Data curation, Formal analysis, Investigation, Methodology, Writing. X.F.: Data curation. H.Z.: Formal analysis. Z.S.: Methodology. J.Z.: Investigation. L.J.: Data curation. Y.L.: Data curation. J.W.: Experiments. X.Z.: Experiments, Data curation, Investigation, Validation, Funding acquisition, Visualization, Editing. Y.Y.: Conceptualization, Project administration, Funding acquisition, Supervision, Editing. All authors reviewed the manuscript.

# **Funding**

The research was supported by the Ningxia Hui Autonomous Region Clinical Medical Research Center for Anorectal Diseases (Integrated Chinese and Western Medicine; grant no. 2022LCZX0013), the Science and Technology Innovation Team of Yinchuan City (grant no. 2022CXTD15), the Science and Technology Program of Yinchuan City (grant no. 2024SF023), and the National Natural Science Foundation of China (Grant no. 82405314).

#### **Declarations**

# Ethics approval and consent to participate

The Ethics Committee of Yinchuan Traditional Chinese Medicine Hospital approved the investigation of clinical samples (2024-98). During the study, we confirm that the informed consent of all participants and/or their legal guardians has been obtained. Research involving human research participants was conducted following the Declaration of Helsinki.

#### Competing interests

The authors declare no competing interests.

# Additional information

**Supplementary Information** The online version contains supplementary material available at https://doi.org/1 0.1038/s41598-025-07889-4.

**Correspondence** and requests for materials should be addressed to X.Z. or Y.Y.

Reprints and permissions information is available at www.nature.com/reprints.

**Publisher's note** Springer Nature remains neutral with regard to jurisdictional claims in published maps and institutional affiliations.

Open Access This article is licensed under a Creative Commons Attribution-NonCommercial-NoDerivatives 4.0 International License, which permits any non-commercial use, sharing, distribution and reproduction in any medium or format, as long as you give appropriate credit to the original author(s) and the source, provide a link to the Creative Commons licence, and indicate if you modified the licensed material. You do not have permission under this licence to share adapted material derived from this article or parts of it. The images or other third party material in this article are included in the article's Creative Commons licence, unless indicated otherwise in a credit line to the material. If material is not included in the article's Creative Commons licence and your intended use is not permitted by statutory regulation or exceeds the permitted use, you will need to obtain permission directly from the copyright holder. To view a copy of this licence, visit <a href="https://creativecommons.org/licenses/by-nc-nd/4.0/">https://creativecommons.org/licenses/by-nc-nd/4.0/</a>.

© The Author(s) 2025